

# Reactions and mass spectra of complex particles using Aerosol CIMS

John D. Hearn, Geoffrey D. Smith\*

*Department of Chemistry, University of Georgia, Athens, GA 30602, USA*

Received 1 May 2006; received in revised form 17 May 2006; accepted 19 May 2006

Available online 27 June 2006

## Abstract

Aerosol chemical ionization mass spectrometry (CIMS) is used both on- and off-line for the analysis of complex laboratory-generated and ambient particles. One of the primary advantages of Aerosol CIMS is the low degree of ion fragmentation, making this technique well suited for investigating the reactivity of complex particles. To demonstrate the usefulness of this “soft” ionization, particles generated from meat cooking were reacted with ozone and the composition was monitored as a function of reaction time. Two distinct kinetic regimes were observed with most of the oleic acid in these particles reacting quickly but with 30% appearing to be trapped in the complex mixture. Additionally, detection limits are measured to be sufficiently low (100–200 ng/m<sup>3</sup>) to detect some of the more abundant constituents in ambient particles, including sulfate, which is measured in real-time at 1.2 µg/m<sup>3</sup>. To better characterize complex aerosols from a variety of sources, a novel off-line collection method was also developed in which non-volatile and semi-volatile organics are desorbed from particles and concentrated in a cold U-tube. Desorption from the U-tube followed by analysis with Aerosol CIMS revealed significant amounts of nicotine in cigarette smoke and levoglucosan in oak and pine smoke, suggesting that this may be a useful technique for monitoring particle tracer species. Additionally, secondary organic aerosol formed from the reaction of ozone with R-limonene and volatile organics from orange peel were analyzed off-line showing large molecular weight products ( $m/z > 300$  amu) that may indicate the formation of oligomers. Finally, mass spectra of ambient aerosol collected offline reveal a complex mixture of what appears to be highly processed organics, some of which may contain nitrogen.

© 2006 Elsevier B.V. All rights reserved.

**Keywords:** Chemical ionization; Organic aerosol; Oleic acid; Wood smoke; Cigarette smoke; Limonene

## 1. Introduction

Aerosols are found throughout the atmosphere and originate from a variety of sources. The source will determine the initial composition of an aerosol affecting the chemical and physical processes in which the particles are involved [1]. Particles that make up aerosols are complex mixtures of perhaps hundreds of compounds [2]. Some of the challenges that face the atmospheric chemistry community are identifying and quantifying individual particle constituents in real time and accurately measuring and predicting particle reactivity. Aerosol mass spectrometry has emerged as an excellent tool for addressing these challenges [3].

Aerosol mass spectrometers vary in their vaporization, ionization, and mass filtering schemes. Thermal vaporization followed by chemical ionization has proven to be an effective

approach to analyzing complex organic particles because of the low degree of fragmentation it offers compared to electron impact or multiphoton ionization [4,5]. This “soft” ionization reduces overlap of ion peaks and simplifies spectra of multi-component mixtures allowing easier measurement of individual species. Chemical ionization has previously been used for studying the kinetics of and products from heterogeneous reactions of one and two component particles [6–8] as well as secondary organic aerosol (SOA) formation in chamber studies [9–11] and the characterization of ambient nanoparticles [12,13]. Unlike other particle mass spectrometers, aerosol chemical ionization mass spectrometry (CIMS) does not remove gas-phase components before analysis, so both gas and particle concentrations can be measured simultaneously. Alternatively, these contributions can be measured separately by using charcoal denuders or filters to remove either volatile organics or particles.

Here we demonstrate both on- and off-line measurements made with Aerosol CIMS to highlight some of the advantages of this technique for analyzing complex aerosols. We first show on-line measurements of laboratory-generated and ambient aerosol

\* Corresponding author.

E-mail address: [gsmith@chem.uga.edu](mailto:gsmith@chem.uga.edu) (G.D. Smith).

to characterize this detection method and demonstrate how it can be used to monitor reactions of complex particles emitted from meat cooking. Then, we use off-line collection of particles to concentrate tobacco and wood smoke, meat cooking aerosol, and non-volatile organic products from gas-phase ozonolysis reactions for analysis by Aerosol CIMS. We also demonstrate how this method can be used to distinguish semi-volatile and non-volatile organics and to analyze ambient aerosol.

## 2. Materials and methods

### 2.1. Chemical ionization mass spectrometry

Primary ions were generated by flowing trace amounts of water vapor or SF<sub>6</sub> in a 3.5 standard liters per minute (slpm) flow of N<sub>2</sub> through a radioactive polonium source (<sup>210</sup>Po, NRD) to generate (H<sub>2</sub>O)<sub>n</sub>H<sup>+</sup> or SF<sub>6</sub><sup>−</sup> ions, respectively [4]. The primary ions were then mixed with the sample flow (1–1.5 slpm), and the sample was chemically ionized by (H<sub>2</sub>O)<sub>n</sub>H<sup>+</sup> or SF<sub>6</sub><sup>−</sup> in a heated (220 °C) 1/2 in. o.d. 24 cm long stainless steel tube. Ions were transmitted into high vacuum through a 100 μm diameter orifice via differential pumping and a small potential gradient (±2 V). Ions were separated using a quadrupole mass filter (ABB Extrel, Pittsburgh, PA, USA) and detected with a channeltron electron multiplier.

#### 2.1.1. On-line measurements

On-line measurements were made by drawing 1.5 slpm of aerosol through a heated glass capillary inlet into vacuum (40 Torr). For ambient sulfate measurements or calibrations the inlet was coupled to conductive tubing. For heterogeneous reactions the inlet was coupled to a 1-m long, 2.54-cm inner diameter (i.d.) glass flow tube. In those experiments, the particles were introduced through a moveable glass injector (1/4 in. o.d.) allowing a variable reaction time of up to 5 s to be achieved [7]. The particles remained on-axis for the length of the flow tube reacting with approximately 100 ppm of ozone before being sampled into the mass spectrometer via the heated glass capillary.

#### 2.1.2. Off-line measurements

Off-line collections of particles were made by pumping 5 slpm of aerosol through a 2-in. section of heated 1/4 in. o.d. stainless steel tube (300 °C) to strip off non-volatile organics. This flow immediately entered a 1/4-in. o.d. stainless steel U-tube (10 in. long) immersed in a cold water bath (0–15 °C) to condense the desorbed organics. Trapped organics were then desorbed directly into the ion tube of the Aerosol CIMS by heating the condensation U-tube wrapped with heating rope to 300 °C over 5.5 min and flowing 1 slpm of N<sub>2</sub> through the tube.

### 2.2. Aerosol generation

Cigarette, white oak, and pine smokes were collected by first igniting the material in a natural gas flame, removing it from the flame and then pumping 5 slpm of the smoke from the burning material through the collection U-tube. Ground beef (20% fat)

was cooked over a natural gas flame, and the generated aerosol was then drawn into an evacuated flask and stored. These stored particles were then swept out with a small flow of N<sub>2</sub> into either the flow tube reactor or the collection U-tube.

The oleic acid particles were created using a glass nebulizer (Meinhard Glass Products), as described in our previous works [4,6]. The mixed oleic acid/palmitic acid particles used to represent meat-cooking aerosol were generated by homogenous nucleation. With this method, small flows of N<sub>2</sub> (100 standard cubic centimeters per minute, sccm) were sent through heated reservoirs (120–130 °C) containing the pure organics and the two organic saturated flows were mixed and heated again (280 °C). The mixed flow was cooled to room temperature, and as the vapors cooled internally mixed particles formed via homogenous nucleation. The polydisperse flow was then sent into an electrostatic classifier (model 3080, TSI, Inc.) to select particles of a particular size (diameter = 700 nm). This method of generating particles eliminates the need to use a volatile solvent, which could alter the chemistry in the particles and made it possible to create particles with solid components, such as palmitic acid.

The ammonium sulfate particles and some of the mixed organic particles were generated through a similar method, called heterogeneous nucleation. With this method, seed particles (diameter <10 nm) were created from the impurities in distilled water by nebulizing the water and then drying it with a diffusion dryer. The resulting seed particles were then sent through heated vapors of ammonium sulfate or the organics, which then condensed onto them. While very similar to homogeneous nucleation, the use of the seed particles in heterogeneous nucleation makes it possible to generate a larger and more stable concentration of particles.

### 2.3. Gases and chemicals

Gases used were N<sub>2</sub> (99.99%, National Welders), O<sub>2</sub> (99.999%, National Welders), and SF<sub>6</sub> (CP grade, Airgas). Ozone was generated by sending O<sub>2</sub> (99.8%, National Welders) through a commercial ozone generator (Pacific Ozone Technology) and either used immediately (orange peel and limonene experiments) or stored on silica gel at −80 °C (flow tube reactions). Chemicals were purchased from Sigma-Aldrich and used without further purification: R-limonene (96%), oleic acid (90%), palmitic acid (99%), lauric acid (99%), ammonium sulfate (100%), and cholesterol (95%). Ground beef (80% lean, 20% fat) was purchased from a local grocery store.

## 3. Results and discussion

### 3.1. On-line measurements

In many situations, on-line analysis of aerosols is advantageous because complications associated with the collection and derivitization of particulate matter can be avoided and particle composition can be monitored in real time. In the following sections, we show results from on-line measurements made with Aerosol CIMS. We begin by calibrating the instrument

for oleic acid and ammonium sulfate, and then we show real-time measurements of ambient condensed-phase sulfate. Finally, using meat-cooking aerosol, we demonstrate how on-line measurements can provide insight into the reactivity of complex particles.

### 3.1.1. Calibration and detection limit for oleic acid

To determine the detection limit of on-line analysis using Aerosol CIMS, the instrument was calibrated with oleic acid particles as a representative organic aerosol. Oleic acid particles were generated by nebulizing the pure liquid into a flask, and then they were swept out of the flask with a small flow of  $N_2$  ( $\sim 10$  sccm) and finally diluted in a 5 slpm flow of  $N_2$ . The resulting particle flow was sampled either into the vaporizer and analyzed with Aerosol CIMS using proton transfer ionization or into an aerodynamic particle sizer (APS model 3321, TSI, Inc.) used to measure the total mass concentration of oleic acid. Fig. 1 shows the sensitivity curve for oleic acid particles, and with a 5-s average and a signal-to-noise of two, we calculate a detection limit of  $200 \text{ ng/m}^3$  ( $4.3 \times 10^8$  molecules/ $\text{cm}^3$ ). This oleic acid detection limit is 25 times lower than the limit that we published previously [4], with the main improvement resulting from the use of a larger-diameter ion tube. The longer reaction time between the  $(H_2O)_nH^+$  reagent ions and the neutral particle vapor in the larger tube makes it possible to detect smaller concentrations within the aerosol.

Despite this improvement, many ambient condensed-phase organics are found at concentrations of only several  $\text{ng/m}^3$  or less [14], so Aerosol CIMS still cannot be used to monitor individual organic species. Further improvements such as real-time particle concentration [15] may help reduce the on-line detection limit of Aerosol CIMS. However, there are other particle constituents at much larger concentrations in the atmosphere that can be detected directly as discussed in the next section.

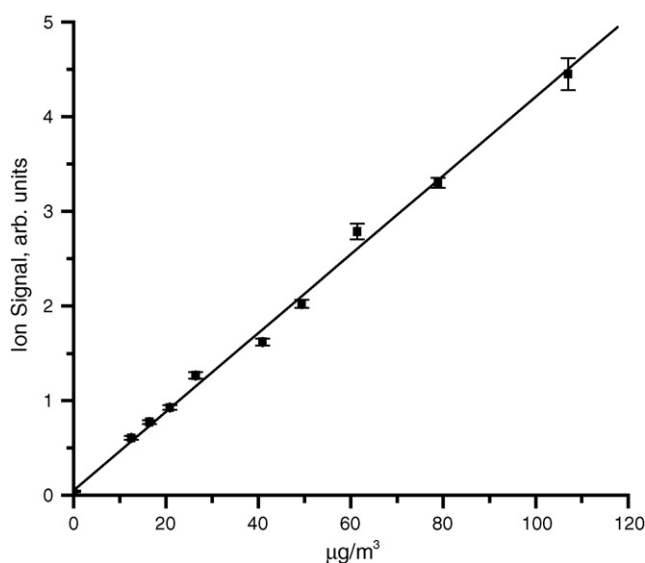


Fig. 1. Calibration curve for oleic acid particles with proton transfer ionization. Concentrations were measured with an aerodynamic particle sizer. The line represents a linear fit to the data yielding a detection limit of  $200 \text{ ng/m}^3$  with  $S/N = 2$ .

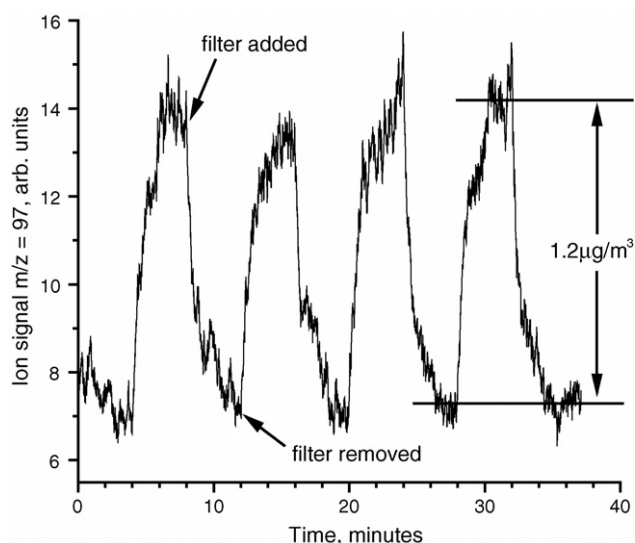


Fig. 2. Data collected from ambient sulfate (detected as bisulfate,  $HSO_4^-$ ) in real time using  $SF_6^-$  as the primary ion. A filter was used to distinguish gas-phase and condensed-phase contributions to the  $m/z = 97$  signal.

### 3.1.2. Detection of ambient sulfate in real time

Sulfate can be found in ambient particles at concentrations of several  $\mu\text{g/m}^3$  [16], and it is expected to be ubiquitous in continental air [17]. Aerosol CIMS may, therefore, be a suitable technique to monitor sulfate concentrations in real time. To test this capability, 6 slpm of outside air was drawn through conductive tubing and 1.5 slpm of this flow was sampled into the mass spectrometer using  $SF_6^-$  to ionize sulfate as  $HSO_4^-$ . A paper filter (300 nm pore size, Whatman Intl.) was either placed in line to remove most (99.99%) of the particles or bypassed to sample particles, thereby separating gas-phase and particle contributions to the signal. Each time the filter was bypassed, the  $HSO_4^-$  signal was seen to double (see Fig. 2), indicating that a significant fraction of sulfate exists on the particles. The large contribution which appears to be from the gas phase has not yet been identified, but it is probably not from sulfuric acid or ammonium sulfate since each of these has a very low vapor pressure. It is possible that an unidentified volatile species with the same mass-to-charge ratio ( $m/z = 97$ ) contributed to the filtered signal.

In order to quantify the ambient sulfate concentration, Aerosol CIMS was calibrated using ammonium sulfate particles generated through heterogeneous nucleation. These particles were either sampled directly into the mass spectrometer or into a scanning mobility particle sizer (model 3936, TSI, Inc.) to measure the total mass concentration. From our calibration (data not shown), we determined that the detection limit for particulate ammonium sulfate is  $100 \text{ ng/m}^3$  and that the observed ambient condensed-phase sulfate concentration was  $1.2 \mu\text{g/m}^3$ . This value is consistent with previous measurements of average particulate sulfate of approximately  $5 \mu\text{g/m}^3$  in nearby Atlanta [16]. We note, however, that the concentration of sulfate measured with Aerosol CIMS may also include contributions from other condensed-phase species, such as sulfuric acid and sodium sulfate [1]. Additionally, the slow response in the signal after the

filter was added may indicate that sulfuric acid or sulfate is sticking to the walls of the tubing or the inlet. While this complication needs to be addressed before quantitative measurements can be made, it is clear that Aerosol CIMS can be used for the real-time monitoring of condensed-phase species that are in a large abundance in the atmosphere.

### 3.1.3. Reactivity of complex organic particles

Aerosol CIMS is particularly well-suited for studying heterogeneous reactions with complex mixtures since the low degree of fragmentation simplifies the spectra. Fewer overlapping peaks make quantitative measurements of a single component possible. Here, as a demonstration of this capability, we present measurements of the kinetics for the reaction of ozone with particles generated from pan frying hamburger meat. Meat-cooking aerosol is known to contain large amounts of fatty acids, and oleic acid and palmitic acid are among the most abundant [14,18]. Recently, the reaction between ozone and oleic acid particles has been studied extensively as a model system representing the oxidation of organic aerosol [7,19–23,24,25,26]. However, it is not clear that the results from these laboratory experiments can be extrapolated to ambient aerosol. In particular, the lifetime of oleic acid in atmospheric particles is predicted to be only minutes based on the reactivity of pure oleic acid droplets, whereas field measurements indicate lifetimes of a few days [20]. In some of the laboratory studies other constituents, such as saturated fatty acids, were found to inhibit the rate of reaction of oleic acid [8,24,25,27], though most of these mixed particles were much simpler than authentic meat-cooking aerosol.

In an effort to better understand the reactivity of more realistic particles, we reacted meat-cooking particles with ozone in the flow tube. Additionally, we reacted pure oleic acid particles and an oleic acid/palmitic acid (OA/PA) mixture to investigate the effect that a solid saturated fatty acid has on oleic acid reactivity. Though meat and meat-cooking aerosol are known to contain several saturated fatty acids, palmitic acid is the most abundant [14,18], and we used it here to represent all of them. Furthermore, since previous studies have found that oleic acid represents approximately 14% of the fatty acids in meat-cooking aerosol [14] and 45% of the fatty acids in intramuscular triacylglycerols in cattle [18], we used a 30/70 (by mole) OA/PA mixture as a simple surrogate. With such a mixture, we were able to study the effect that the palmitic acid, which is mostly solid (from the phase diagram measured by Inou et al. [28]), has on the reactivity of the liquid oleic acid. While we have previously shown that similar mixtures containing oleic acid and *n*-alkanoic acids can exist as supercooled droplets [8], we determined that the OA/PA particles used here were not supercooled.

Fig. 3 shows the fractional reaction decay of oleic acid as a function of exposure to ozone ( $P_{O_3} \cdot t$ ) for each of the three types of particles. On the timescale of the experiments (5 s), the oleic acid in the pure particles reacts quickly and to completion (<1% remaining), while in both the binary mixture and the meat-cooking particles a significant fraction (15–30%) is unreacted. These observations indicate that some of the oleic acid in the mixed particles reacts quickly but that some of it is inhibited from reacting with  $O_3$  suggesting that it may be “trapped”. While

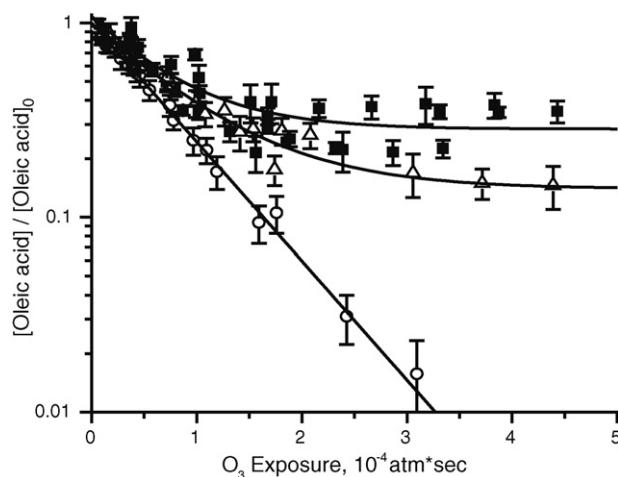


Fig. 3. Reaction of oleic acid with ozone in pure oleic acid particles (open circles), oleic acid/palmitic acid particles ( $X_{oleic}=0.3$ , open triangles), and oleic acid in meat cooking particles (filled squares). Pure oleic acid reacts to completion, but the two mixtures show evidence of significant trapping of oleic acid. Lines are drawn to guide the eye.

similar observations of trapping in particles containing solid *n*-alkanoic acids have also been noted recently [8,24,25,27], this appears to be the first study in which such a behavior has been observed in authentic meat-cooking aerosol. Extrapolation of these results to a polluted atmosphere (i.e., 100 ppb  $O_3$ ) suggests that some of the oleic acid will have a short half-life (i.e., several minutes), while the rest will have a much longer half-life (several hours to days). Consequently, trapping by solid constituents (such as *n*-alkanoic acids) does appear to occur in primary source particles and could reconcile the long ambient lifetimes inferred from field measurements.

Finally, we point out that while the signal at  $m/z = 283$  might comprise contributions from other species, this seems unlikely since the only other identified organic with the same molecular weight is 5-tetradecyldihydro-2(3H)-furanone, and it is not abundant enough to account for the 30% of unreacted signal [14]. Therefore, we conclude that the reaction of oleic acid with ozone is, indeed, inhibited in the complex meat-cooking particles.

### 3.2. Off-line measurements

While Aerosol CIMS is well suited to monitor heterogeneous reactions and to detect some ambient condensed phase species that are in large abundance, it still lacks the detection capability necessary to make real time measurements of individual organic compounds in the atmosphere. Additionally, while the ability to measure volatile, semi-volatile, and non-volatile components simultaneously is sometimes advantageous, it can make it difficult to differentiate gas-phase and particle sources. To better characterize particulate emissions from several primary sources and to improve detection for ambient measurements with Aerosol CIMS, we have developed a simple procedure for the offline collection and concentration of particles. With this approach, particle components are desorbed at 300 °C, condensed and collected in a cold U-tube (0–15 °C) and then desorbed and analyzed with Aerosol CIMS. In the sec-



tions that follow, we first characterize this method of collection with known mixtures and then present spectra from several primary sources and one secondary source of aerosol. Finally, we demonstrate the usefulness of this approach for analyzing ambient aerosol.

### 3.2.1. Collection efficiency and desorption profiles

To determine the collection efficiency of the desorption/condensation method for sampling organic particles, we generated 180 nm internally mixed particles containing oleic acid, palmitic acid, and myristic acid via heterogeneous nucleation. The particle mass spectra were then monitored in real time using Aerosol CIMS both before and after the aerosol passed through the U-tube collection apparatus (data not shown). The signal for each component decreased by 90% when the particles were sent through the U-tube indicating that the collection efficiency for these components is high. These observations suggest that this procedure may be a convenient method for concentrating non-volatile organics from particles. However, there will be a collection bias against components that have extremely low volatilities, such as ammonium sulfate which melts at 280 °C, and indeed we only collect 25% of the sulfate with this technique. While this bias makes quantification difficult, this method can still be valuable in identifying condensed-phase components on particles.

The desorption of the collected organics from the U-tube also provides an additional dimension of analysis since they are expected to evolve according to their vapor pressures as the temperature is increased. This capability was tested under controlled conditions using small amounts ( $\approx 500$  ng) of lauric acid, palmitic acid, oleic acid, and cholesterol which were simultaneously deposited in the collection tube and desorbed into the mass spectrometer. Fig. 4 shows the total normalized integrated signal for each species (detected as the  $[M+H]^+$  ion) as the

desorption temperature was increased from 25 °C to 300 °C. While vapor pressure data is not available for each of these species over this range of temperatures, it can be seen that they desorb in the order of their melting and boiling points: lauric acid (mp = 44 °C, bp = 298 °C), palmitic acid (mp = 62 °C, bp = 339 °C), oleic acid (mp = 16 °C, bp = 360 °C), and cholesterol (mp = 147 °C, bp = 360 °C) [29]. Lauric acid is seen to desorb first, even though its melting point is higher than that of oleic acid (44 °C versus 16 °C), because it has a much lower boiling point (and thus a higher vapor pressure at the same temperature). Palmitic acid is seen to desorb next, followed by oleic acid and then cholesterol. Despite the fact that the boiling point for cholesterol is identical to that of oleic acid, it probably desorbs at much higher temperatures because its melting point is so much higher (147 °C versus 16 °C). Not only are these desorption profiles useful in separating various components of the concentrated aerosol, but they may also be used for differentiating two species of the same molecular weight if they have sufficiently different vapor pressures.

### 3.2.2. Meat cooking aerosol

Off-line collection was used to record mass spectra of emissions from panfrying ground beef. Fig. 5A shows a mass spectrum using proton transfer ionization of the collected aerosol as it is desorbed from the tube. This mass spectrum is a “snapshot” of the organics as they desorb from the collection tube. Several of the prominent peaks correspond to organic acids, which as a class, comprise a large fraction of the total organic aerosol emitted from cooking ground beef [14,30]. In particular, peaks at  $m/z$  = 145, 159, 173, 187, 255, 257, and 283 correspond to octanoic acid, nonanoic acid, decanoic acid, undecanoic acid, palmitoleic acid, palmitic acid, and oleic acid, respectively. There may be contributions to these signals from other species, but the organic acids listed above are

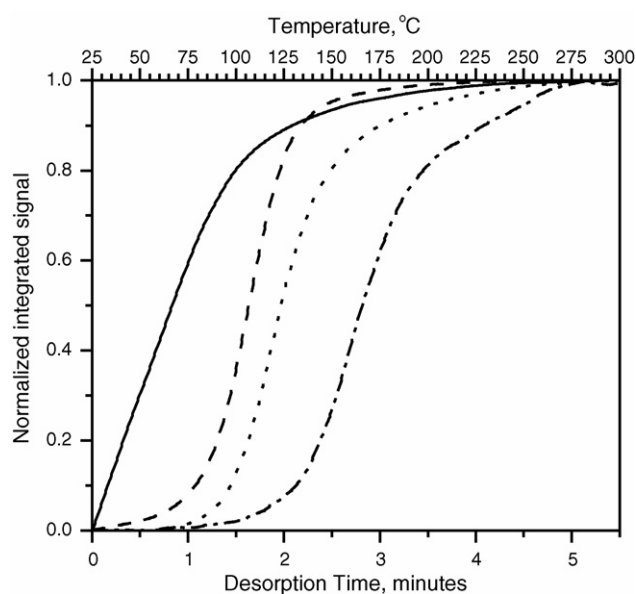


Fig. 4. Normalized integrated desorption profiles for lauric acid (solid line), palmitic acid (long dash), oleic acid (short dash), and cholesterol (long-short) desorbed in order of increasing vapor pressures.

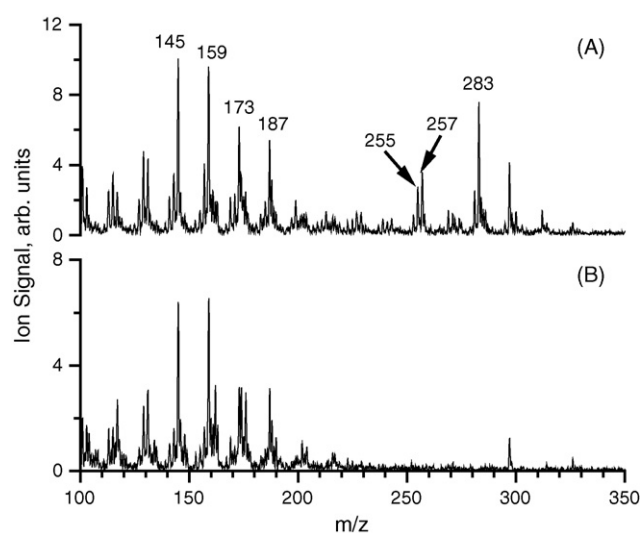


Fig. 5. Mass spectra of collected meat-cooking aerosol with the particles either (A) heated to 300 °C or (B) not heated prior to entering the cold (0 °C) collection U-tube. The non-volatile components ( $m/z > 220$  amu) are only detected when desorbed prior to collection (A), but semi-volatile components are seen in both spectra.

expected to be the major contributors at those mass-to-charge ratios.

The collection may also be used to distinguish between non-volatile and semi-volatile species simply by adjusting the desorption temperature at the inlet to the U-tube. When this inlet is not heated, semi-volatiles may still be collected in the cold condensation tube, but non-volatiles will remain on the particles and will not be collected. However, when the inlet is heated to 300 °C both non-volatiles and semi-volatiles will be collected. To demonstrate this separation capability, meat-cooking aerosol was sent through two collection U-tubes simultaneously: one in which the inlet was heated to 300 °C and the other in which the inlet was kept at room temperature. The components with lower molecular weight that are expected to have a higher vapor pressure are still trapped in the collection tube with the unheated inlet (Fig. 5B), but higher molecular weight species ( $m/z > 220$  amu) are only evident in the spectrum for which the inlet was heated (Fig. 5A). Of course, it is not possible to quantify the fraction of the semi-volatile organics on the particles with this type of measurement, but it does allow them to be differentiated from the non-volatile components.

### 3.2.3. Tobacco and wood smoke

Smoke from cigarette, white oak, and pine combustion was also analyzed off-line using Aerosol CIMS. Fig. 6 shows two snapshots of the desorption of collected cigarette smoke. Panel A shows the mass spectrum before the collection tube was heated (semi-volatile organics), showing significant amounts of nicotine ( $m/z = 163$ ), consistent with its room-temperature vapor pressure of 42.5 mTorr [31] and previous observations that it is found both in the gas-phase and on particles [32]. Panel B shows the mass spectrum after a few minutes of heating the collection U-tube. There is signal at every mass unit, which is not surprising considering the complexity of the emitted aerosol [33]. Some of the larger peaks in the mass spectrum ( $m/z = 111, 124, 147, 163$ , and 177 amu) correspond to organic compounds that have been identified previously as condensed-phase components in

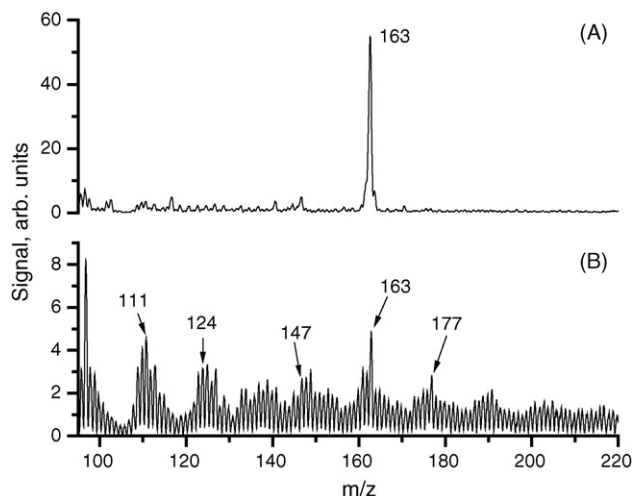


Fig. 6. Mass spectra for collected cigarette smoke (A) before the collection U-tube was heated and (B) while the collection U-tube was heated.

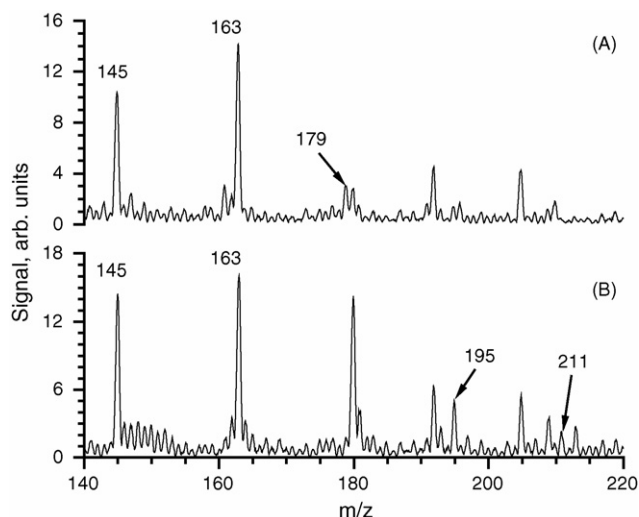


Fig. 7. Mass spectra from collected (A) pine and (B) white oak wood smoke. Levoglucosan ( $m/z = 163$ ), a common tracer for wood smoke, can be seen in both spectra.

cigarette smoke (benzenediol, nicotinic acid, myosmine, nicotine, and cotinine, respectively) [33].

Fig. 7 shows a snapshot of the desorption of aerosol collected from burning pine (panel A) and white oak (panel B) woods. The dominant peak in both spectra is from levoglucosan ( $m/z = 163$ ) which is a particle tracer for biomass burning [34]. Peaks at  $m/z = 195$  and 211 probably correspond to methoxyeugenol and syringyl acetone, respectively. Both of these organics are expected to be emitted in larger abundance from white oak combustion than pine [35,36]. Additionally, a peak at  $m/z = 179$  is present in larger relative abundance in the pine smoke spectrum than white oak and could be from coniferyl aldehyde [36]. The large peak at  $m/z = 145$  is most likely a fragment peak from levoglucosan (water loss). Of course, there may be contributions to these peaks from other organic species, but these two spectra appear to be representative of the two sources based on previous source characterization from oak and pine combustion.

### 3.2.4. Secondary organic aerosol

Secondary organic aerosol (SOA) makes up a significant fraction of ambient particulate mass, and the reaction of ozone with terpenes, such as  $\alpha$ -pinene or limonene, can be an important source of SOA [37]. R-limonene is the primary terpene emitted from orange peel [38], and along with other emitted terpenes, it reacts with ozone to form low-volatility products [10,39,40] that can form new particles [41,42]. In some cases, limonene originating from cleaning products can react with ozone and also be an important source of particulate matter indoors with potential health impacts [43]. To characterize the particle products from this reaction using Aerosol CIMS, we filled a 500-mL flask with ozone and inserted a piece of orange peel or a drop of R-limonene, after which particles were immediately visible by eye. The aerosol was then swept out with a small flow of  $O_2/O_3$ , collected in the U-tube and the products were then desorbed and analyzed via Aerosol CIMS (Fig. 8).

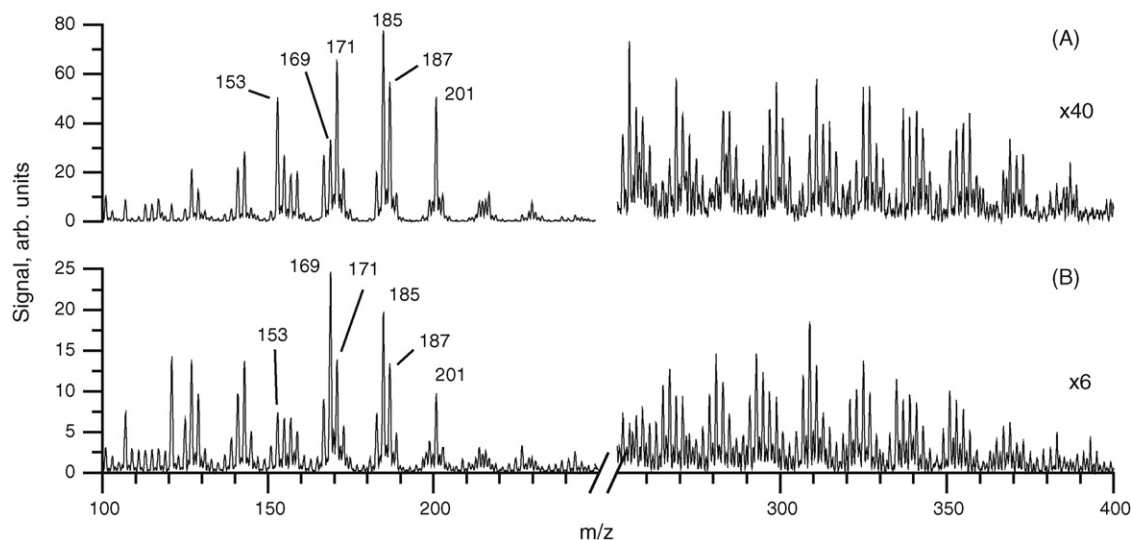


Fig. 8. Mass spectra from the reaction of ozone with (A) volatile compounds from orange peel and (B) R-limonene. Large molecular weight products ( $m/z > 250$  amu) suggest the formation of oligomers.

Many of the prominent peaks in the reacted orange peel spectrum (Fig. 8A) are also present in the reacted R-limonene spectrum (Fig. 8B), consistent with the fact that it is the dominant volatile organic emitted from oranges. Peaks at  $m/z = 169$ , 171, 185, 187, and 201 correspond to products that have been observed previously for R-limonene ozonolysis (limonaldehyde, limonic acid, limononic acid, limonic acid, and 7-hydroxy-limononic acid, respectively) [40]. In addition to these expected products, higher molecular weight products ( $m/z = 250$ –400) are visible in the spectra of both the orange peel and R-limonene reactions suggesting that oligomers may be formed. While these products cannot be identified conclusively from the mass spectra, the soft vaporization and ionization afforded by Aerosol CIMS keep these large molecular weight species intact with relatively little fragmentation compared to many other ionization methods. Such large molecular weight products have been observed previously in other systems, including  $\alpha$ -pinene ozonolysis [44–48], and was very recently reported for limonene ozonolysis [49].

### 3.2.5. Ambient sampling

This off-line collection method also allows concentration of ambient aerosol making it possible to detect organics that otherwise would be below the detection limit. Fig. 9 shows a mass spectrum obtained by drawing outside air ( $1.8 \text{ m}^3$ ) through the U-tube for 6 h and then desorbing and analyzing the collected particulate matter with Aerosol CIMS. Peaks are present at nearly every mass unit above 100 amu with progressions of peaks evident every 14 amu corresponding to sequentially larger organics with additional  $-\text{CH}_2-$  groups (see hash marks at top of Fig. 9). These species probably include mono- and di-carboxylic acids, aldehydes, ketones, alcohols, alkenes and dienes, as well as multi-functional species such as keto-acids and hydroxy keto-acids, all of which would be detected through the proton-transfer ionization used here. We note that any alkanes present would not be detected since they are very inefficiently ionized [4]. Interest-

ingly, a similar progression of ion peaks from ambient aerosol collected in Germany has also been reported recently using a soft vacuum-UV ionization approach [50].

Close inspection of the spectrum in Fig. 9 reveals peaks at even mass-to-charge ratios that are quite pronounced suggesting a large presence of nitrogen-containing organics, such as alkylamines [51] or organic nitrates. These peaks are not nearly as large in the spectra of the reacted orange peel and R-limonene (Fig. 8) in which the peaks alternate in intensity between the even and odd mass-to-charge ratios. This sort of alternating pattern is expected for a complex mixture of organics in the absence of amines and nitrates. Because agriculture is prevalent in the areas surrounding Athens, Georgia, it is not surprising that amines

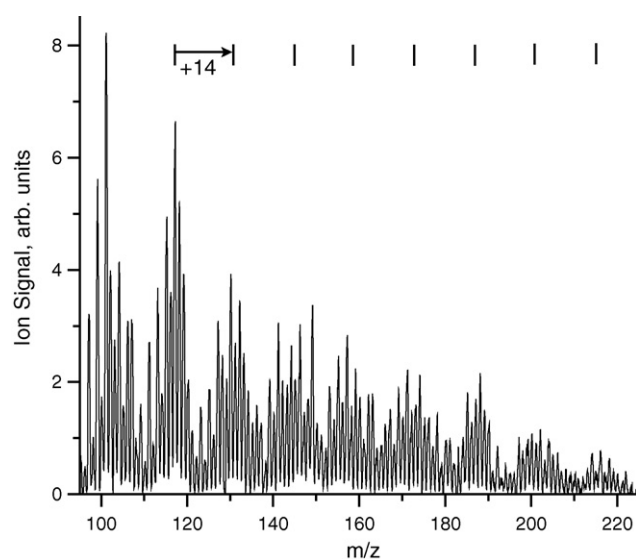


Fig. 9. A mass spectrum from ambient aerosol collected in Athens, Georgia. Notice the progression of peaks every 14 amu (hash marks) indicating a complex mixture of organics. The abundant peaks at even mass-to-charge ratios suggest possible contributions from nitrogen-containing organics.

may be found in the collected particulate matter. Additionally, the presence of a wastewater treatment plant only a mile from the sampling site may be a significant source of amines [52]. Furthermore, low-volatility products from the reaction of NO<sub>3</sub> with volatile organics, especially important at nighttime, could be a source of organic nitrates in the atmosphere [53,54].

While the mass spectra of ambient aerosol collected with Aerosol CIMS are complicated and the features cannot be assigned definitively, the soft ionization may provide additional insight into their compositions. Additionally, MS/MS experiments using chemical ionization can provide fragmentation and offer further information on the structure and identities of organics [10]. The Aerosol CIMS technique also provides detection limits for organic species, which are comparable to others which are currently used, such as thermal desorption gas-chromatography mass spectrometry (TD-GCMS) and solvent extraction followed by analysis with GC-MS. For example, we measure a detection limit of 4 ng for oleic acid deposited in the U-tube, whereas Ho et al. report detection limits of 1–4 ng for a variety of *n*-alkanes using TD-GCMS and 40–125 ng using solvent extraction followed by GC-MS. Both Aerosol CIMS and TD-GCMS can be used to detect a wide variety of organic molecules without the complication of extraction. Furthermore, Aerosol CIMS can be used without derivitization which can be especially useful for species such as organic acids.

There are currently a number of limitations, however, associated with using the U-tube for collecting particles. First of all, there is a size bias because the mass spectrometer signal will be dominated by large particles (>1 µm), but this could be improved rather simply by adding an impactor or a cyclone to the inlet. There are also uncertainties in the collection efficiencies for various particulate species making quantification difficult. Additionally, collection of 1.8 m<sup>3</sup> of aerosol at 5 slpm takes 6 h making it difficult to observe fast temporal variability in the aerosol composition. Future improvements will include optimization of the desorption/collection in the U-tube at sampling rates of up to 50 slpm, thereby reducing the sampling time to approximately half an hour. We will also use this approach to find specific tracer species which may be used to identify local particle sources and to determine the significance of alkylamines and organic nitrates in ambient aerosol.

#### 4. Conclusions and future direction

Aerosol CIMS is a powerful tool for studying laboratory-generated particles and heterogeneous reactions, and steps have been taken to apply this technique for characterizing ambient aerosol. The low degree of fragmentation makes it possible to analyze complex aerosol and measure the reactivity of individual organics in a multi-component mixture. We have shown that some of the oleic acid in meat-cooking particles reacts quickly with ozone, but that some of it appears to be “trapped” or isolated from reaction. This difference may explain the long lifetimes of some particle constituents in the atmosphere (i.e., days) inferred from field measurements. On-line detection limits for this technique are sufficiently low (100–200 ng/m<sup>3</sup>) that it can be used

to measure laboratory-generated particles and some ambient condensed-phase species in real-time (e.g., sulfate).

The off-line desorption/condensation collection procedure makes it possible not only to concentrate aerosol but also to differentiate semi-volatile and non-volatile organic species during collection and analysis with Aerosol CIMS. Abundant particle tracer species, such as levoglucosan from wood smoke, are shown to be easily detected from primary emissions using this approach. Large molecular weight products ( $m/z > 300$  amu) are detected in secondary organic aerosol formed from the ozonolysis of R-limonene because of the low degree of fragmentation possible with chemical ionization.

Finally, ambient aerosol was collected and analyzed using Aerosol CIMS yielding mass spectra with peaks at nearly every mass-to-charge ratio below  $m/z = 220$  amu demonstrating the complexity of the particles. Progressions of peaks spaced by 14 amu indicate series of functionalized organic species, and prominent peaks at even mass-to-charge ratios suggest the presence of nitrogen-containing species. Improvements in the collection procedure should make it possible to reduce the sampling time thereby making it easier to monitor temporal variations in particle composition.

#### Acknowledgments

We gratefully acknowledge support from the National Science Foundation (ATM-0402226) and the American Chemical Society Petroleum Research Fund.

#### References

- [1] B.J. Finlayson-Pitts, J.N. Pitts, *Chemistry of the Upper and Lower Atmosphere: Theory, Experiments, and Applications*, Academic Press, San Diego, 2000, 969 pp.
- [2] W.F. Rogge, L.M. Hildemann, M.A. Mazurek, G.R. Cass, B.R.T. Simoneit, *Environ. Sci. Technol.* 32 (1998) 13–22.
- [3] C.A. Noble, K.A. Prather, *Mass Spectrom. Rev.* 19 (2000) 248–274.
- [4] J.D. Hearn, G.D. Smith, *Anal. Chem.* 76 (2004) 2820–2826.
- [5] B. Warscheid, U. Kueckelmann, T. Hoffmann, *Anal. Chem.* 75 (2003) 1410–1417.
- [6] J.D. Hearn, G.D. Smith, *J. Phys. Chem. A* 108 (2004) 10019–10029.
- [7] J.D. Hearn, A.J. Lovett, G.D. Smith, *Phys. Chem. Chem. Phys.* 7 (2005) 501–511.
- [8] J.D. Hearn, G.D. Smith, *Phys. Chem. Chem. Phys.* 7 (2005) 2549–2551.
- [9] T. Hoffmann, R. Bandur, U. Marggraf, M. Linscheid, *J. Geophys. Res. (Atmos.)* 103 (1998) 25569–25578.
- [10] B. Warscheid, T. Hoffmann, *Rapid Commun. Mass Spectrom.* 15 (2001) 2259–2272.
- [11] B. Warscheid, T. Hoffmann, *Atmos. Environ.* 35 (2001) 2927–2940.
- [12] D. Voisin, J.N. Smith, H. Sakurai, P.H. McMurry, F.L. Eisele, *Aerosol Sci. Technol.* 37 (2003) 471–475.
- [13] J.N. Smith, K.F. Moore, F.L. Eisele, D. Voisin, A.K. Ghimire, H. Sakurai, P.H. McMurry, *J. Geophys. Res. (Atmos.)* 110 (2005) D22S03.
- [14] W.F. Rogge, L.M. Hildemann, M.A. Mazurek, G.R. Cass, B.R.T. Simoneit, *Environ. Sci. Technol.* 25 (1991) 1112–1125.
- [15] M.D. Geller, S. Biswas, P.A. Fine, C. Sioutas, *J. Aerosol Sci.* 36 (2005) 1006–1022.
- [16] A.J. Butler, M.S. Andrew, A.G. Russell, *J. Geophys. Res. (Atmos.)* 108 (2003) 8415.
- [17] S.-H. Lee, D.M. Murphy, D.S. Thomson, A.M. Middlebrook, *J. Geophys. Res. (Atmos.)* 107 (2002) 4003.
- [18] M. Itoh, C.B. Johnson, G.P. Cosgrove, P.D. Muir, R.W. Purchas, *J. Sci. Food Agric.* 79 (1999) 821–827.



- [19] T. Moise, Y. Rudich, *J. Phys. Chem. A* 106 (2002) 6469–6476.
- [20] J.W. Morris, P. Davidovits, J.T. Jayne, J.L. Jimenez, Q. Shi, C.E. Kolb, D.R. Worsnop, W.S. Barney, G. Cass, *Geophys. Res. Lett.* 29 (2002) L014692.
- [21] G.D. Smith, E. Woods III, C.L. DeForest, T. Baer, R.E. Miller, *J. Phys. Chem. A* 106 (2002) 8085–8095.
- [22] T.D. Thornberry, J.P.D. Abbatt, *Phys. Chem. Chem. Phys.* 6 (2004) 84–93.
- [23] Y. Katrib, S.T. Martin, H.-M. Hung, Y. Rudich, H. Zhang, J.G. Slowik, P. Davidovits, J.T. Jayne, D.R. Worsnop, *J. Phys. Chem. A* 108 (2004) 6686–6695.
- [24] D.A. Knopf, L.M. Anthony, A.K. Bertram, *J. Phys. Chem. A* 109 (2005) 5579–5589.
- [25] P.J. Ziemann, *Faraday Discuss.* 130 (2005) 469–490.
- [26] J. Zahardis, B. LaFranchi, G. Petrucci, *J. Geophys. Res. (Atmos.)* 110 (2005), doi:10.1029/2004JD005336.
- [27] Y. Katrib, G. Biskos, P.R. Buseck, P. Davidovits, J.T. Jayne, M. Mochida, M.E. Wise, D.R. Worsnop, S.T. Martin, *J. Phys. Chem. A* 109 (2005) 10910–10919.
- [28] T. Inoue, Y. Hisatsugu, R. Ishikawa, M. Suzuki, *Chem. Phys. Lipids* 127 (2004) 161–173.
- [29] R.L. Brown, S.E. Stein (Eds.), “Boiling Point Data” in NIST Chemistry WebBook, NIST Standard Reference Database Number 69 (<http://webbook.nist.gov>). P.J. Linstrom, W.G. Mallard (Ed.), National Institute of Standards and Technology, Gaithersburg, MD, 2006.
- [30] J.D. McDonald, B. Zielinska, E.M. Fujita, J.C. Sagebiel, J.C. Chow, J.G. Watson, *J. Air Waste Manage. Assoc.* 53 (2003) 185–194.
- [31] L.B. Norton, C.R. Bigelow, W.B. Vincent, *J. Am. Chem. Soc.* 62 (1940) 261–264.
- [32] J.F. Pankow, *Chem. Res. Toxicol.* 14 (2001) 1465–1481.
- [33] W.F. Rogge, L.M. Hildemann, M.A. Mazurek, G.R. Cass, *Environ. Sci. Technol.* 28 (1994) 1375–1388.
- [34] B.R.T. Simoneit, J.J. Schauer, C.G. Nolte, D.R. Oros, V.O. Elias, M.P. Fraser, W.F. Rogge, G.R. Cass, *Atmos. Environ.* 33 (1999) 173–182.
- [35] J.J. Schauer, M.J. Kleeman, G.R. Cass, B.R.T. Simoneit, *Environ. Sci. Technol.* 35 (2001) 1716–1728.
- [36] P.M. Fine, G.R. Cass, B.R.T. Simoneit, *Environ. Eng. Sci.* 21 (2004) 705–721.
- [37] J.J. Chen, R.J. Griffin, *Atmos. Environ.* 39 (2005) 7731–7744.
- [38] D.V. Mccalley, J.F. Torresgrifol, *Analyst* 117 (1992) 721–725.
- [39] T. Hoffmann, J.R. Odum, F. Bowman, D. Collins, D. Klockow, R.C. Flagan, J.H. Seinfeld, *J. Atmos. Chem.* 26 (1997) 189–222.
- [40] S. Leungsakul, M. Jaoui, R.M. Kamens, *Environ. Sci. Technol.* 39 (2005) 9583–9594.
- [41] J.M. Andino, T.J. Wallington, M.D. Hurley, R.P. Wayne, *J. Chem. Educ.* 77 (2000) 1584–1586.
- [42] A.M. Jonsson, M. Hallquist, E. Ljungstrom, *Environ. Sci. Technol.* 40 (2006) 188–194.
- [43] T. Wainman, J.F. Zhang, C.J. Weschler, P.J. Liroy, *Environ. Health Perspect.* 108 (2000) 1139–1145.
- [44] M.P. Tolocka, M. Jang, J.M. Ginter, F.J. Cox, R.M. Kamens, M.V. Johnston, *Environ. Sci. Technol.* 38 (2004) 1428–1434.
- [45] Y. Iinuma, O. Boge, T. Gnauk, H. Herrmann, *Atmos. Environ.* 38 (2004) 761–773.
- [46] U. Baltensperger, M. Kalberer, J. Dommen, D. Paulsen, M.R. Alfarra, H. Coe, R. Fisseha, A. Gascho, M. Gysel, S. Nyeki, M. Sax, M. Steinbacher, A.S.H. Prevot, S. Sjoren, E. Weingartner, R. Zenobi, *Faraday Discuss.* 130 (2005) 265–278.
- [47] R. Bahreini, M.D. Keywood, N.L. Ng, V. Varutbangkul, S. Gao, R.C. Flagan, J.H. Seinfeld, D.R. Worsnop, J.L. Jimenez, *Environ. Sci. Technol.* 39 (2005) 5674–5688.
- [48] D.S. Gross, M.E. Galli, M. Kalberer, A.S.H. Prevot, J. Dommen, M.R. Alfarra, J. Duplissy, K. Gaeggeler, A. Gascho, A. Metzger, U. Baltensperger, *Anal. Chem.* 78 (2006) 2130–2137.
- [49] C. Mueller, Y. Iinuma, O. Boege, H. Herrmann, *Geophys. Res. Abstr.* 8 (2006) 02538.
- [50] T. Ferre, F. Muhlberger, R. Zimmermann, *Anal. Chem.* 77 (2005) 4528–4538.
- [51] S. Angelino, D.T. Suess, K.A. Prather, *Environ. Sci. Technol.* 35 (2001) 3130–3138.
- [52] S.E. Manahan, *Environmental Chemistry*, sixth ed., CRC Press, Inc., Boca Raton, FL, 1994.
- [53] I. Wangberg, I. Barnes, K.H. Becker, *Environ. Sci. Technol.* 31 (1997) 2130–2135.
- [54] M. Hallquist, I. Wangberg, E. Ljungstrom, I. Barnes, K.H. Becker, *Environ. Sci. Technol.* 33 (1999) 553–559.